STUDIA UBB CHEMIA, LVI, 3, 2011 (p. 5 - 13)

MORPHO-STRUCTURAL CHARACTERIZATION OF TiO_2 NANOSIZED POWDERS WITH PHOTOCATALYTIC POTENTIAL

MONICA BAIA[a], MONICA SCARISOREANU[b], ION MORJAN[b], IULIANA P. MORJAN[b], LUCIAN BAIA[a], VERONICA COSOVEANU[c], RODICA ALEXANDRESCU[b], VIRGINIA DANCIU[c]

ABSTRACT. Anatase/rutile mixed nanopowders were obtained by laser pyrolysis technique and the influence of the flow rate of the oxidizing agent on their morpho-structural properties was explored by transmission electron microscopy (TEM), X-ray diffraction (XRD) and Raman spectroscopy. The revealed particularities were comparatively discussed with those of the commercial product Degussa P-25 from the perspective of the photocatalytic performances.

Keywords: *TiO_2 nanosized powders, morphological investigations, structural properties*

INTRODUCTION

The efficient treatment of industrial wastewaters and contaminated drinking water sources has became of great importance in a world that is facing ever increasing population and decreasing energy resources. An ideal waste treatment process will completely mineralize all the toxic species present in the waste stream without leaving behind any hazardous residues [1]. It should also be cost-effective. At the current phase of development, none of the treatment technologies approach this ideal situation.

Catalytic applications of TiO_2 have been studied for decades regarding the elimination of environmental pollutants because of its stability and non-toxicity. TiO_2 is the most investigated photocatalyst because it ensures efficient degradation of pollutants from air, water and soil. The band gap of this semiconductor is ca. 3.2 eV, corresponding to a radiation of wavelength around 380 nm [2]. Therefore, UV light is needed to excite the electrons

[a] *Babes-Bolyai University, Faculty of Physics, M. Kogalniceanu 1, 400084 Cluj-Napoca, Romania, monica.baia@phys.ubbcluj.ro*
[b] *National Institute for Lasers, Plasma and Radiation Physics, P.O.Box MG-36, Bucharest-Magurele, Romania*
[c] *Babes-Bolyai University, Faculty of Chemistry and Chemical Engineering, A. Janos 11, 400028 Cluj-Napoca, Romania*

from the valence band to the conduction band. The generated electron-hole pairs serve as the oxidizing and reducing agents. The photodegradation of pollutants in water takes place due to the ·OH radicals, which are formed either through the interaction of water molecules with a hole or through the interaction of oxygen molecules with hot electrons, which are the key active species [3].

Since Gleiter's report [4] on nano-materials, more attention was directed towards the research of nanoparticles. It is known that the efficiency of TiO_2 is influenced by factors like crystalline structure [5], particle size [5, 6], and preparation methods [7]. There are many methods for preparing TiO_2 nanoparticles such as: sol-gel method, ball milling, chemical vapor deposition and microemulsion [7]. In a previous study [8] the synthesis of TiO_2 mixed nanopowders using the laser pyrolysis technique as a single-step reaction route was successfully reported. $TiCl_4$ and air were used as gas-phase precursors. Moreover, the influence of the laser power and the flow rate of the oxidizing agent of the samples structure was investigated, for certain synthesis parameters [9]. The photocatalytic performances of these materials were also assessed and the results showed that this preparation method is promising for producing highly active TiO_2 nanopowders [10].

In this work we propose to further explore the morpho-structural properties of this type of TiO_2 nanosized powders from the photocatalytic performance perspective. The influence of the air flows on the morphological and structural properties is analyzed, at a certain C_2H_4 flow through $TiCl_4$. As compared to previously analyzed samples [8-10], different values of the Ar confinement flow and Ar flow for windows cleaning were used in the synthesis of the powders under investigation. The morphology, crystalline structure and particle size were evaluated by transmission electron microscopy (TEM), X-ray diffraction (XRD) and Raman measurements and, the samples structural particularities were comparatively discussed with those of the commercial product Degussa P25.

RESULTS AND DISCUSSION

Prior to investigating the samples, which were coded SC 1-4 and SC 6, energy dispersive analysis by X-rays (EDAX) was performed and the elemental content is summarized in Table 1. One should note that the SC 6 sample was obtained with an increased air flow rate, as described in the Experimental section.

From Table 1 one can observe that a pronounced contamination with carbon occurs in both samples, in principal, due to the high amount of ethylene sensitizer decomposition. The presence of quasi-amorphous carbon in the environmental matrix was also observed in previous laser pyrolysis experiments [11, 12].

Table 1. Elemental content of the TiO_2 nanopowders.

Samples code	C At%	O At%	Cl At%	Ti At%
SC 1-4	60.29	23.71	4.47	11.54
SC 6	72.78	16.79	0.99	9.44

Ethylene sensitizer is not always chemically inert and could undergo various extents of dissociation. The favorable conditions for C_2H_4 dissociation mainly rely on the existence of a strong oxidizing atmosphere during titania gas-phase synthesis. This adventitious carbon is almost totally eliminated by heating the samples in air at rather low temperatures (about 250 ^oC). One can also notice the chlorine presence in both samples as a by-product of the synthesis reaction. However, with increasing the air flow rate (sample SC 6) the chlorine amount is more than four times smaller due to the accelerated $TiCl_4$ dissociation (see Table 1).

XRD measurements were further performed and the diffractogramms are illustrated in Figure 1. Both patterns exhibit a background located at small 2θ values due to the amorphous structure presence. The coexistence of anatase and rutile phases was identified.

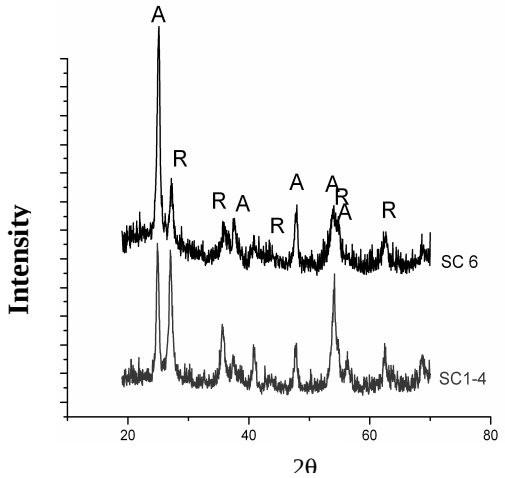

Figure 1. X-ray diffraction patterns of the TiO_2 nanopowders**. A** and **R** denote the anatase and rutile phases.

The estimations of the weight percentage of both phases, on the relative crystallized titania amount together with the crystallites mean size calculated according to the Scherrer's formula by considering the peaks

located around $2\theta=25^0$ are given in Table 2. For comparison purpose the commercial product Degussa P-25 was also investigated.

As can be observed from Table 2, different amounts of crystalline phases are developed inside the samples. Thus, in the case of the SC 1-4 sample the rutile phase is preponderantly formed, while in the SC 6 sample the anatase phase is the main developed crystalline phase. Previous studies reported [9, 13] about the effect of carbon coating in stabilization of the anatase phase. By taking into account the data summarized in Table 1 related to the carbon content, one can assume that the formation of the anatase phase in the sample SC 6 as the main phase could be associated with the existence of a higher amount of carbon.

Table 2. Structural parameters of the TiO_2 nano-powders as estimated from XRD analysis

Samples code	TiO_2 crystalline phase content (%)		Crystallites dimension (nm)		Specific surface area (m^2/g)
	A	R	A	R	
SC 1-4	42	58	20	16	81
SC 6	75.5	24.5	17	14	86
Degussa P-25	80	20	~ 20	~ 30	50

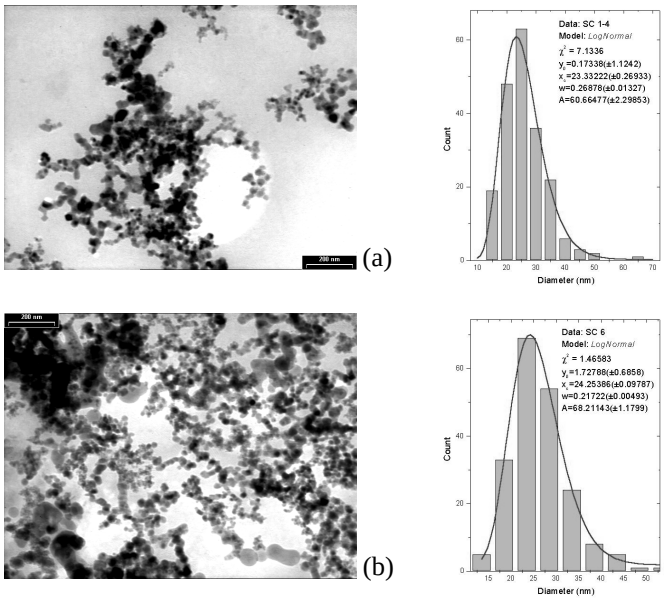

Figure 2. TEM micrographs of the TiO_2 nanopowders and the corresponding particle size distributions:(a) SC 1-4 and (b) SC 6.

By looking at the data from Table 2, related to the specific surface area of the pores, one can see small differences between these values. Therefore, one can infer that this morphological parameter cannot influence the photocatalytic potential of the prepared samples.

TEM micrographs of TiO_2 samples (Figure 2) show bunches of loosely-bound aggregated nanoparticles. The sharp particle distributions of the samples make easier the assessment of the mean diameter values that were found to be of ~ 25 and 23 nm and for the samples SC 1-4 (Figure 2a) and SC 6 (Figure 2b), respectively. Thus, with increasing the air flow the nanoparticles dimension decreases, in agreement with previously reported results [9]. However, the nanoparticles dimensions are higher than those of the before prepared samples [10], most probably due to the different synthesis conditions. As expected, an important difference related to the crystallites dimension between the data derived from TEM images and those obtained from XRD analysis exists. However, the mean sizes of the crystallites determined by TEM follow the same logic with those obtained by XRD, i.e. higher dimensions for SC 6 than for SC 1-4.

In order to get further insight into the nanoparticles' morphology TEM images in high resolution mode were also recorded and are presented in Figure 3. The polyhedral shapes and amorphous interfaces of nanoparticles are well noticeable. Thus, in the case of SC 1-4 sample (Figure 3a), an almost squared nanoparticle with lateral dimension of about 12 nm is displayed. The SC6 sample mainly contains elongated nanoparticles, with dimensions of about 30 nm in length and about 20 nm wide. Some ordered defects can be also observed at the nanoparticles interface (see the inset from Figure 3b).

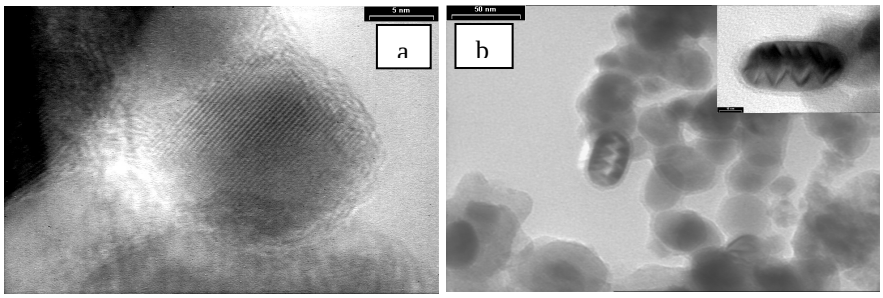

Figure 3. TEM micrographs in high resolution mode obtained from the TiO_2 nanopowders**:** SC 1-4 (a) and SC 6 (b).

The Raman spectra of the laser pyrolyzed TiO_2 nanopowders are illustrated in Figure 4 and show only two distinct peaks that can be associated with the carbon presence. The first one, located near 1350 cm^{-1} (D-band), is

attributed to the A_{1g} mode and is due to the in-plane disorder [14-16]. This band originates from the disorder-induced scattering generated by imperfections or loss of hexagonal symmetry in the carbon structures [16]. The second Raman characteristic is often present in all carbon and graphite materials spectra around 1595 cm^{-1} (G-band), and is associated with the $2E_{2g}$ mode. By looking at the above mentioned features one observes that the overall Raman signal given by carbon is more intense in the spectrum of sample SC 6 in comparison with that observed in the spectrum of sample SC 1-4. On the other hand, by analyzing the intensities ratio of the two bands it seems that the amorphous/crystalline ratio is not significantly modified as a result of the changes performed in the samples preparation. It should be mentioned that no signature of the anatase or rutile phase was evidenced in the recorded Raman spectra. Taking into consideration that these crystalline structures possess a high Raman sensitivity, i.e. their cross section is high, one can certainly infer that the carbon content is extremely high, as previously was found.

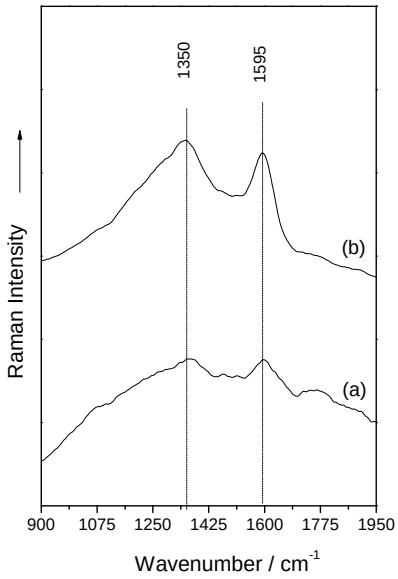

Figure 4. Raman spectra of the TiO_2 nanopowders:(a) SC 1-4 and (b) SC 6.

The revealed structural properties can be considered favorable from the perspective of the photocatalytic activity. Thus, from the viewpoint of the anatase phase formation, the best photocatalytic performance is expected from the sample with the highest anatase content, SC 6. On the contrary, the observed differences between the crystallites dimension achieved for the investigated samples and commercial product Degussa P-25 seem to indicate

a better photocatalytic potential for the SC 1-4 sample. However, although the specific surface area is a key parameter in the photocatalytic assessments, it does not completely influence the performance. Thus, another important parameter that certainly influences this evaluation of the photocatalytic properties is the carbon amount. Therefore, the higher carbon content found inside the sample SC 6 in comparison with SC 1-4 would certainly lead to a decrease of its photocatalytic performances. In order to further improve the samples photocatalytic performances a heat treatment that will eliminate the amorphous carbon should be applied.

CONCLUSIONS

Anatase/rutile mixed nanopowders have been obtained by laser pyrolysis and the influence of the flow rate of the oxidizing agent on their morpho-structural properties was evaluated from the perspective of photocatalytic applications. TEM, XRD and Raman spectroscopy were the complementary techniques used for this purpose and the results have been compared with those of the commercial product Degussa P-25, a well known photocatalyst. A substantial increase of the rutile to anatase phase ratio in comparison to Degussa P-25 powder was obtained when a reduced air flow was used, and the presence of a structure preponderantly of anatase was observed when the air flow was higher. One should also emphasize that the high carbon content present inside the prepared samples could be an important drawback in the improvement of the photocatalytic performances.

EXPERIMENTAL SECTION

Samples preparation

The samples were prepared by the laser synthesis technique with the help of a pyrolysis set-up elsewhere described [8], in which $TiCl_4$ and air are simultaneously allowed to emerge into the flow reactor. Ethylene served as a carrier for the $TiCl_4$ vapors and as an energy transfer agent. The used experimental parameters are displayed in Table 3.

Table 3. Experimental parameters for the TiO_2 nanopowders. Note the different values of the air flow used for the samples preparation.

Samples code	ϕ Ar_f [sccm]	ϕ Ar_{conf} [sccm]	ϕ Air [sccm]	ϕ C_2H_4 +$TiCl_4$ [sccm]	P [mbar]	P_{Laser} [W]
SC 1-4	300	1100	50	100	450	200
SC 6	300	1100	75	100	450	200

slm – standard litre per minute, sccm – standard cubic centimetres per minute

Samples characterization

The elemental composition was evaluated from X-ray energy dispersive analysis (EDAX) performed with a SEM-EDX Philips apparatus, using 15 kV acceleration voltage, 1000x magnification and 200 s acquisition time. The surface area of the synthesized samples was determined by using a Sorptomatic 1990 equipment and N_2 adsorption. The specific surface area was obtained by the BET method. The XRD patterns were collected on a PANalytical X'Pert MPD theta–theta system in continuous scan mode (counting 20 s/0.02 2h) between $2\theta = 20–90^o$. A Ni filter, a curved graphite monochromator and a programmable divergence slit (enabling constant sampling area irradiation) were positioned in the diffracted beam ($\lambda = 0.15418$ nm). The powdery deposits were imaged in a transmission electron microscope (TEM) Philips CM120ST (Customized Microscope 120 Super Twin, 120 kV max acceleration voltage, about 2 A resolution, C_S=~1.2 mm). The samples were also analyzed by high resolution TEM (HRTEM). The Raman spectra of the samples were recorded by using a Witec confocal Raman system CRM 200 equipped with a 100x/0.8 microscope objective and a 300 lines/mm grating. In the recording of the spectra the 633 nm laser line with a power of 3 mW and a spectral resolution around 5 cm^{-1} were employed.

ACKNOWLEDGMENTS

Monica Baia would like to thank for the financial support of the Sectoral Operational Programme for Human Resources Development 2007-2013, co-financed by the European Social Fund, under the project number POSDRU/21/1.5/G/36154 with the title „Performant doctoral program for the development of highly qualified human resources in the interdisciplinary scientific research".

REFERENCES

1. D. F. Ollis and H. Al-Ekabi (Eds.) "Photocatalytic Purification and Treatment of Water and Air", Elsevier, Amsterdam, **1993**.
2. M. Gratzel, "Photocatalysis: Fundamentals and Applications", N. Serpone, E. Pelizzetti (eds.) Wiley, New York, **1989,** 123.
3. H. Al-Ekabi, N. Sperpone, E. Pelizzetti, C. Minero, M. A. Fox, R. B. Draper, *Langmuir,* **1989,** *5***,** 250.
4. H. Gleiter, *Prog. Materials Science,* **1989**, *33*, 223.
5. K. Tanaka, T. Hisanaga, A. P. Rivera, "Photocatalytic Purification and Treatment of Water and Air" D. F. Ollis, H. Al-Ekabi (eds.), Elsevier, Amsterdam, **1993,** 169.

6. Z. Zhang, C. C. Wang, R. Zakaria, J. Ying, *Journal of Physical Chemistry B,* **1998***, 102*, 10871.
7. N. Serpone, D. Lawless, R. Khairutdinov, *Journal of Physical Chemistry,* **1995***, 99***,** 16655.
8. R. Alexandrescu, F. Dumitrache, I. Morjan, I. Sandu, M. Savoiu, I. Voicu, C. Fleaca, R. Piticescu, *Nanotechnology* **2004**, *15***,** 537.
9. M. Scarisoreanu, Morjan, R.Alexandrescu, R. Birjega, I. Voicu, C. Fleaca, E. Popovici, I. Soare, L. Gavrila-Florescu, O. Cretu, V.Ciupina, E. Figgemeier, *Applied Surface Science* **2007**, *253*, 7908.
10. E. Figgemeier, W. Kylberg, E. Constable, M. Scarisoreanu, R. Alexandrescu, I. Morjan, I. Soare, R. Birjega, E. Popovici, C. Fleaca, L. Gavrila-Florescu, G. Prodan, *Applied Surface Sci*ence **2007**, *254*, 1037.
11. I. Morjan R. Alexandrescu, I. Soare, F. Dumitrache, I. Sandu, I. Voicu, A. Crunteanu, E. Vasile, V. Ciupina, S. Martelli, *Materials Science Engineering C* **2003**, *23,* 211.
12. I. Morjan, R. Alexandrescu, F. Dumitrache, R. Birjega, C. Fleaca, I. Soare, C. R. Luculescu, G. Filoti, V. Kuncer, L. Vekas, N. C. Popa, G. Prodan, *Journal of Nanoscience and Nanotechnology*, **2010**, *10*, 1223.
13. M. Inagaki, F. Kojin, B. Tryba, M. Toyoda, *Carbon* **2005**, *43*, 1652.
14. F. J. Maldonado-Hodar, C. Moreno-Castilla, J. Rivera-Utrilla, Y. Hanzawa, Y. Yamada, *Langmuir* **2000**, *16*, 4367.
15. G. A. M. Reynolds, A. W. P. Fung, Z. H. Wang, M. S. Dresselhaus, R. W. Pekala, *Journal of Non-Crystalline Solids* **1995**, *188,* 27.
16. L. C. Cotet, M. Baia, L. Baia, I. C. Popescu, V. Cosoveanu, E. Indrea, J. Popp, V. Danciu, *Journal of Alloys & Compounds* **2007**, *434–435*, 854